

General Disclaimer

One or more of the Following Statements may affect this Document

- This document has been reproduced from the best copy furnished by the organizational source. It is being released in the interest of making available as much information as possible.
- This document may contain data, which exceeds the sheet parameters. It was furnished in this condition by the organizational source and is the best copy available.
- This document may contain tone-on-tone or color graphs, charts and/or pictures, which have been reproduced in black and white.
- This document is paginated as submitted by the original source.
- Portions of this document are not fully legible due to the historical nature of some of the material. However, it is the best reproduction available from the original submission.

**NASA TECHNICAL
MEMORANDUM**

NASA TM 73,163

**(NASA-TM-73163) FLIGHT TEST RESULTS OF THE
STRAPDOWN HEXAD INERTIAL REFERENCE UNIT
(SIRU). VOLUME 1: FLIGHT TEST SUMMARY
(NASA) 27 p HC A03/MF A01 CSCL 17G**

N77-26111

**Unclas
G3/04 31775**

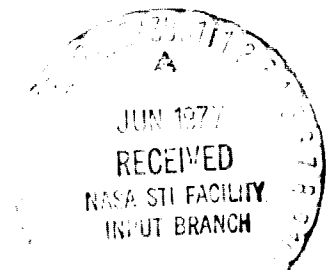
NASA TM 73,163

**FLIGHT TEST RESULTS OF THE STRAPDOWN HEXAD INERTIAL
REFERENCE UNIT (SIRU)
VOLUME I: FLIGHT TEST SUMMARY**

Ronald J. Hruby and William S. Bjorkman

**Ames Research Center
Moffett Field, Calif. 94035**

June 1977



1. Report No. NASA TM 73,163	2. Government Accession No.	3. Recipient's Catalog No.	
4. Title and Subtitle FLIGHT TEST RESULTS OF THE STRAPDOWN HEXAD INERTIAL REFERENCE UNIT (SIRU) VOLUME I: FLIGHT TEST SUMMARY		5. Report Date	
		6. Performing Organization Code	
7. Author(s) Ronald J. Hraby and William S. Bjorkman*		8. Performing Organization Report No. A-5924	
9. Performing Organization Name and Address Ames Research Center Moffett Field, Calif. 94035		10. Work Unit No. 513-53-05	
		11. Contract or Grant No.	
12. Sponsoring Agency Name and Address National Aeronautics and Space Administration Washington, D. C. 20546		13. Type of Report and Period Covered Technical Memorandum	
		14. Sponsoring Agency Code	
15. Supplementary Notes *Analytical Mechanics Associates, Inc. Mountain View, California 94040			
16. Abstract Results of flight tests of the Strapdown Inertial Reference Unit (SIRU) navigation system are presented. The fault-tolerant SIRU navigation system features a redundant inertial sensor unit and dual computers. System software provides for detection and isolation of inertial sensor failures and continued operation in the event of failures. Flight test results include assessments of the system's navigational performance and fault tolerance.			
17. Key Words (Suggested by Author(s)) Strapdown inertial navigation Redundancy management, fault-tolerance Aircraft navigation		18. Distribution Statement Unlimited STAR Category - 04	
19. Security Classif. (of this report) Unclassified	20. Security Classif. (of this page) Unclassified	21. No. of Pages 25	22. Price* \$3.25

FLIGHT TEST RESULTS OF THE STRAPDOWN HEXAD INERTIAL REFERENCE UNIT (SIRU)

VOLUME I: FLIGHT TEST SUMMARY

Ronald J. Hrubby and William S. Bjorkman*

Ames Research Center

SUMMARY

A flight test program was conducted by NASA Ames Research Center to evaluate the performance of the redundant, modularized, fault-tolerant Strapdown Inertial Reference Unit (SIRU) in an aircraft environment. The results of the flight test program are described in three volumes. This document, Volume I, summarizes the findings of the program. Volume II contains a detailed description of the flight test program and its results. Volume III contains appendixes which expand on relevant particulars of the SIRU system and the flight test program.

The principal flight test objectives included assessment of:

1. SIRU system performance as an unaided inertial navigation system
2. Capability of system redundancy management software to detect sensor failures
3. Flight performance of the dual computer configuration

The results of 15 separate flights showed that the unaided inertial navigation accuracy during cruise was better than 3 n. mi./hr error growth. During terminal area maneuvers, these errors were less than 5 n. mi./hr. Such error growths are tolerable for short-haul operation where flight times are short and where radio navigation updates are available. Additional analysis, design, and testing would reduce these error growths further. Updating the inertial data with recorded Distance Measuring Equipment (DME) readings (post-flight) enabled the theoretically aided system to bound the error within 0.2 n.mi.

The flight test showed that with the existing SIRU design it was possible to isolate gyro failures equal to or greater than $1.6^\circ/\text{hr}$. A detection threshold set to detect failures less than $1.6^\circ/\text{hr}$ would result in excessive false alarms. A gyro failure of $1.6^\circ/\text{hr}$ is considered to be a hard failure from the standpoint of unaided navigation. From the standpoint of flight control, it represents a very soft failure.

*Senior Analyst, Analytical Mechanics Associates, Inc., Mountain View, California.

The fault detection and isolation algorithms are the area in need of most research for the overall SIRU concepts to become operational in aircraft. The SIRU dual computer system provided both reliable and correct information. However, several design improvements which could improve the overall reliability and maintainability of a future system are suggested.

INTRODUCTION

Current avionics systems employ numerous sensors, actuators, and display devices for various flight modes. These systems often overlap in function, and therefore, a limited degree of control and navigation reliability is provided by this redundancy. However, redundancy, when implemented, most often provides reliability by way of hardware duplication. For example, in commercial aircraft application, where inertial navigation system reliability is considered necessary for operational success, redundancy has been implemented by triplicate systems. An integrated, redundant, avionic implementation with self-contained fault identification and adaptation capabilities is clearly needed for future aircraft operations to eliminate unnecessary backup configurations (ref. 1). Advances in sensors and semiconductor technology, coupled with advances in redundant navigation, guidance, and control computer algorithms, have made possible the Strapdown Inertial Reference Unit (SIRU). The SIRU is a redundant, modularized, fault-tolerant system originally developed for space applications by the Charles Stark Draper Laboratory under Contract NAS9-8242 with NASA Johnson Space Center (refs. 2 and 3). Under Contract NAS2-7439 with NASA Ames Research Center, the original laboratory mechanization was modified to provide a flightworthy, redundant navigation system installed in the NASA Convair 340 (CV-340) aircraft (refs. 4 and 5). The SIRU Flight Test Program was undertaken by NASA Ames Research Center to evaluate SIRU in an aircraft flight environment. The primary goal of the SIRU Flight Test Program was to develop a baseline for the performance of an integrated guidance, navigation, and flight control system for short-haul aircraft.

The SIRU Flight Test System is a free-inertial (unaided, dead-reckoning) navigation system consisting of a strapdown hexad inertial sensor array and dual computers. The sensors consist of six single-degree-of-freedom integrating gyros and six linear accelerometers. The six sensing axes of the inertial sensor array lie along the normals to six nonparallel faces of an imaginary dodecahedron illustrated in figure 1. Each axis contains one integrating rate gyro module (IRIG 1 & MOD B) and one accelerometer module (16PM PIP MOD B).

The SIRU dodecahedron configuration and redundancy management software permit the navigation system to function when any three gyros and any three accelerometers are operational. This is contingent upon faulty sensors being detected and removed. When sensor failures are detected and the faulty sensor identified (isolated), outputs of the faulty sensors are excluded from the computation of position, velocity, and attitude by system software. The system continues to function with the remaining sensors. The modular features embodied in the SIRU system include prealigned, normalized, interchangeable assemblies in which each instrument is integrated with its own torque loop and

temperature controller. The remaining electronics are located in interchangeable modules, by axis, in the electronics assembly section. The modular feature enhances system maintenance repair and line replacement unit capability.

It should be noted that the gyros used in the SIRU are experimental precision-floated gyros. These gyros are not strong candidates for strapdown applications in short-haul aircraft because of high cost, warmup time required, and calibration requirements. However, much of the functional software and many of the redundancy management techniques evaluated in this program are generic to strapdown navigation systems in general and provide a basis for further investigations using other sensor concepts, such as laser or tuned rotor gyros.

SIRU was exercised in a laboratory environment from July 1970 through July 1974, prior to the adaptation of the SIRU instrument package for flight tests. Fifteen flight tests of the SIRU system were made in NASA's CV-340 aircraft between May 20, 1975 and September 24, 1975. The flight test system had a digital tape recorder for recording flight test data on magnetic tape and plasma information displays. The installation of SIRU in the CV-340 is shown in figure 2.

Several navigational references were utilized in the flight test program to evaluate navigational performance. In addition to the two Nike-Hercules radars operated by NASA at the Crows Landing NALF test facility, the test program utilized (a) multiple station DME data from a digitally tuned DME receiver, (b) optical waypoint position fixes taken on landmarks with a driftmeter and recorded by camera, and (c) surveyed position benchmarks with latitude and longitude used as external references. Barometric and radar altitude were also measured and recorded in flight. The position references were not used in the free-inertial navigation computations except for initialization purposes.

This summary document discusses the primary objectives of the flight test program, describes the flight test program and the aircraft position reference system, and summarizes the flight test results, including navigation accuracy performance of the failure detection and isolation algorithms, and hardware and software limitations.

SIRU FLIGHT TEST OBJECTIVES

The broad goal of the SIRU Flight Test Program was to explore the feasibility of achieving low-cost, highly reliable, short-haul navigation, guidance and control through application of strapdown inertial systems technology and redundancy management techniques. This goal was attained by flight testing the SIRU system in the NASA Ames CV-340 aircraft. This evaluation provided a performance baseline for future integrated strapdown, redundant-component aircraft guidance, navigation, and flight control systems. The tests also provided the basis for projecting navigational performance, fault detection, and isolation threshold requirements for aircraft flight control and navigation.

The principal flight test objectives included assessment of:

1. System performance as a skewed-sensor, free-inertial navigational system, as evidenced by navigational accuracy achieved in the flight tests
2. System capability to detect and isolate sensor failures by way of redundancy management software
3. The performance of the dual computer configuration and its compatibility with the hexad sensor redundancy concept

The last objective included combining the flight results with laboratory results (refs. 5 and 6). Secondary objectives of the test program included (a) the determination of DME and Nike-Hercules radar accuracies for calibration of the aircraft position reference system, (b) development of data reduction procedures, and (c) an assessment of SIRU's inertially smoothed radio navigation potential.

FLIGHT TEST PROGRAM DESCRIPTION

The SIRU Flight Test Program began May 20, 1975, and ended on September 24, 1975. Several acceptance flights were made earlier at Hanscom Field, Massachusetts, near Boston (ref. 5). A total of 15 flights was made, with 3 devoted entirely to assessment of cruise navigation performance.

All flights were made in California's San Joaquin and Salinas Valleys, shown in figure 3. The landmarks (waypoints) used for visual calibration of the reference system are depicted in figure 3. In general, triangular courses were followed with Crows Landing used as the central, calibrated waypoint. The largest segmented courses included Sacramento, Modesto, Salinas, Moffett Field, and Oakland as waypoints.

Two types of flight test patterns were flown: enroute (Moffett to Crows Landing and return), and terminal area (in the vicinity of Crows Landing). The enroute patterns were similar to the one illustrated in figure 4. This shows takeoff from Moffett Field, turning to fly over the Moffett DME for a tape mark, flying over the San Jose DME for another tape mark, flying over Lick Observatory for a visual mark, overflying the Crows Landing DME for a final tape mark, and then landing. Portions of each of the flights were utilized for test calibration and system adjustments. Most flights were made below 3000-m (10,000-ft) altitude. Cruise flights were of sufficient length to record one or more complete Schuler periods.

Terminal area maneuver tests followed a flight profile similar to the one illustrated in figure 5. The flight tests generally combined both enroute and terminal segments.

A typical flight sequence originating at Crows Landing after a fine alignment is shown in figure 6. In this flight, the CV-340 left Crows Landing,

crossed Stockton, Modesto, Castle AFB, Merced, and finally turned back to Crows Landing. At each waypoint, a visual calibration was made by using the driftmeter and marking the time of passing runway reference points. The time of the waypoint mark was automatically recorded on the magnetic tape for post-flight correlation with the SIRU and reference system's data.

Position Reference System

The position reference system used during the SIRU flight tests to track the CV-340 aircraft consisted of three primary references: (a) the NASA radar tracking system at Crows Landing NALF, California, (b) a multiple DME system mounted within the aircraft, and (c) time-referenced photographs of airport reference benchmarks taken periodically from the CV-340 throughout each flight. The radar tracking system consisted of two modified Nike-Hercules radar systems. The modification provided improved resolution through the use of 19-bit range and angle digital shaft encoders. No atmospheric refraction correction was provided. A transponder aboard the CV-340 was used to improve angle tracking.

The multiple DME receiver system provided range information from as many as six DME stations. The system utilized a fast-switching DME receiver which was automatically programmed to scan sequentially for each of six selectable DME frequencies. Range lockup time was 1 sec maximum, and range output resolution was 18.5 m (0.01 n. mi.).

Photographs of reference landmarks were taken from the aircraft by a camera mounted on a standard military driftmeter installed in the underside of the aircraft fuselage. The positions of the driftmeter and multiple-DME system within the CV-340 are illustrated in figure 2. The time point at which each photograph was taken was recorded in the SIRU digital tape recorder in order to correlate with radar and DME position data. The number of photographs per flight varied from 8 to 16 depending upon the length of the flight. The driftmeter's level gyro was inoperable during most of the flight tests, thus introducing a small amount of uncertainty in the aircraft position as determined from the photographs.

The relative accuracies of the different methods of locating the aircraft position are summarized in table 1. This table lists the rms residuals obtained from combinations of radar/photograph (driftmeter), DME/photograph, and radar/DME. The residuals listed in table 1 are much smaller than the SIRU navigation errors sustained during the flight tests.

TABLE 1.- POSITION REFERENCE SYSTEM RMS RESIDUAL SUMMARY

Average residual, m		
Radar photograph	DME photograph	Radar DME
135.23	220.19	218.65

The software for analyzing the SIRU flight test data, using the Ames IBM 360 and CDC 7600 computers, is presented in Volume II of this report.

FLIGHT TEST RESULTS

Summary

The flight tests included multiple segments in which each segment produced a magnetic tape of recorded SIRU test data. In most cases, SIRU was fine-aligned between segments, so that each such segment could be considered a separate flight test. Thirty-four segments were flown, producing about 36 hr of navigation data. Commentary on individual flights is found in Volumes II and III of this report.

Figure 7 depicts the in-flight duration, navigation mode duration, and radar coverage for the 15 flight tests; the flight date appears on the left of the figure. Each flight segment is represented by an unbroken horizontal line. Later segments are shown relative to the zero time point of the first segment for each multisegment flight. Navigation duration for any segment is indicated by the length of the segment's unbroken line. The darkened portion of the line indicates time in flight, with "T" denoting takeoff and "L" denoting landing. Radar coverage periods are indicated by parenthesized line segments just above the navigation segments. Observe that 12 of the 15 flights had some radar coverage. DME coverage, although of less accuracy than radar coverage, was present in almost unbroken fashion for every flight test segment.

Table 2 summarizes characteristics of the Ames Research Center flight tests. Navigation mode and flight duration (in seconds) are listed after a brief description of the route flown by the CV-340. "Radar intersection" is a tabulation of the total time interval during which there are data concurrently on both the SIRU and radar tapes. The column headed "Marks" contains the number of position fixes taken and recorded; "Computers" identifies which computers were recorded and whether they differed when both were recorded; "Rate" denotes whether raw sensor data were recorded at the high rate "H" (20 Hz) or the low rate "L" (1 Hz).

Maximum position error is shown in nautical miles and, in most cases, refers to the DME-derived position, which was assumed to be correct. The maximum error usually occurred at the end of the recorded segment. It should be noted that some tests were flown without particular concern for navigational accuracy and that operational mistakes are included with the "errors."

Detected failures are listed in the last two columns of table 2. Failure, in the context of this report, means that the performance of a given instrument, gyro or accelerometer, exceeded a predetermined limit that had been established in the failure detection software. Unscheduled failures are those which were unintentional, while scheduled failures were caused by intentionally miscompensating the sensors at some point in flight. The notation "G(FCBDEA)," for example, indicates that every gyro failed at some time during the test, the order of failure being first F and finally A. The notation A(D) means that only accelerometer D failed during the segment.

TABLE 2.- FLIGHT TEST SUMMARY

Flight data	Route	Navigation duration, sec	Flight duration, sec	Radar intersection, sec	Marks	Computers	Rate	Maximum position error, n. mi.	Detected failures	Unscheduled (a)	Scheduled (a)
5/20	Moffett/Crows	5170	2230	1655	6	B	L	5.93	G(CF)		--
5/30A	Moffett/Crows	2300	1285	0	9	B	H	12.82	G(FCBDEA), A(A)		--
5/30B	Crows/Los Banos/Moffett	5980	4390	2295	23	B	H,L	41.02	G(EFABCD)		--
6/16A	Moffett/Crows	3074	1608	0	11	A=B	L	23.08	G(FCEABD), A(AD)		--
6/16B	Crows/Moffett	2321	1670	0	8	A=B	L	3.55	G(ABPCED), A(E)		--
6/18	Moffett/Sac./Moffett	15303	14185	0	30	A	L	33.99	G(EACBF), A(D)		--
6/25	Crows/Crows	3405	2450	3282	10	A=B	H	12.94	G(CDBA)A(D)		--
7/14	Moffett/Stockton/Moffett	6005	4323	0	11	B	H	35.59	G(BDACP)		--
7/17A	Moffett/Stockton	5956	4000	1020	14	A	H	4.40	--		--
7/17B	Stockton/Moffett	4155	3925	3085	12	A	H	2.10	--	G(CA)	--
7/24A	Moffett/Crows	2400	1295	354	6	A=B	H	2.79	--		--
7/24B	Crows/Stockton/Crows	2555	2163	2447	5	A=B	H	1.23	--	A(CE)	--
7/24C	Crows/Stockton/Crows	2587	2241	2417	6	A=B	H	4.04	--	A(CA),A(C)	--
7/28A	Moffett/Stockton/Crows	3971	3439	3174	9	A=B	H	14.06	G(FBE)	G(CD)	--
7/28B	Crows/Moffett	2426	1392	1469	8	A=B	H	7.13	G(E)	G(C) ^b	--
8/22A	Moffett/Crows	2630	1181	553	7	A=B	H	2.93	--		--
8/22B	Crows/Crows	2110	646	2038	6	A=B	H	.36 ^c	G(E),A(E)	G(AB)	--
8/22C	Crows/Bakersfield	4082	3422	2566	5	A=B	VH,L	11.16	G(EF),A(E)	G(AB)	--
8/22D	Bakersfield/Moffett	--	4320	--	6	A	H	--	G(E),A(A)		--
8/29A	Moffett/Crows	2620	1202	850	6	A=B	H	7.65	--	G(BA)	--
8/29B	Crows/Crows/Crows	2501	553	2316	5	A=B	H	.3 ^c	--	G(BA)	--
9/05A	Moffett/Crows	2200	1231	0	6	A=B	H	2.50	G(A)	G(FE)	--
9/05B	Crows/Crows	3067	1990	1774	2	A=B	H	3.72	G(F)	A(BA)	--
9/05C	Crows/Crows	2331	1498	1404	2	A=B	H	1.86	G(F)	G(E)	--
9/05D	Crows/Moffett	2053	1369	1497	6	A=B	H	3.00	G(EF)	A(DC)	--
9/10A	Moffett/Crows	3750	2467	1758	4	A=B	H	3.97	--		--
9/10B	Crows/Crows(A cont'd)	2527	1794	2365	5	A=B	H	10.19	G(B)		--
9/10C	Crows/Crows(B cont'd)	2652	1952	2459	6	A=B	H	19.36	--		--
9/10D	Crows/Moffett(C cont'd)	1859	1187	0	4	A=B	H	20.14	--		--
9/18A	Moffett/Crows	3860	2890	2173	4	A=B	H	6.22	--		--
9/18B	Crows/Crows(A cont'd)	3045	2415	3045	5	A=B	H	7.62	--		--
9/18C	Crows/Crows(B cont'd)	2690	2467	2690	5	A=B	H	6.88	--		--
9/18D	Crows/Moffett	1600	1091	804	5	A=B	H	2.91	G(FE),A(E)		--
9/24	Moffett/Baker/Moffett	15819	14293	8928	21	A=B	L	7.8	--		--

^aIt should be noted that the large number of failures through most of the early flights were caused by low TSE limits and procedural problems. During later flights, some unscheduled failures were detected and resolution of the cause not determined. G(FCBDEA) indicates gyros F, C, B, D, E, and A failed in that order. A(A) indicates accelerometer A failed, etc.

^bSmall failure undetected (below detection limit).

^cPosition and velocity were re-set during navigation.

Navigation Accuracy Results

Navigation accuracy was evaluated by comparing the indicated position with a position independently derived from one of the external position references at the same computer frame time.

Except for occasional bad data intervals, the external position references were in good agreement during the SIRU test program. Discrepancies from the references were small relative to the system navigational error. In each instance where the B computer differed from the A computer (by the insertion of scheduled failures into B and not into A), the navigational error estimate from the better computer (A) was used in performance calculations.

Table 3 summarizes navigation performance during the flight test program. The maximum position error (residual) appears after the flight date and navigation duration columns. This maximum error does not necessarily occur at the end of the navigation segment because the navigational error does not grow linearly with time. In an attempt to represent the navigational error as a simple function of time, the navigation error was "fitted" by the least-squares method to:

1. a constant (the average, shown in column 4 of the table)
2. a straight line through the origin (slope is shown in column 5)
3. a straight line (error = $a + bt$, as shown in column 6, b in column 7)

The data in table 3 show generally improved navigational performance with time into the test program, and wide variations in navigational performance between segments of particular flights.

On the basis of table 3, system navigational accuracy rating at the end of the test program was about 3 to 4 n. mi./hr. although flight 9/24 indicated 1.02 n. mi./hr. The wide variations between same-day segments were due to alignment uncertainties and human error because bias and scale-factor sensor output correction were common among these segments. The variations were also caused by the effects of different maneuvers on dynamic sensor compensations.

Failure Detection and Isolation (FDI) Algorithm Performance

The SIRU failure detection algorithm is based upon computing the sum total of the squared error (TSE) of each inertial sensor type and comparing it against a dynamically changing threshold called maximum allowed squared error (MASE). When the TSE exceeds the threshold by a certain ratio, a sensor fault is indicated. Setting the threshold too low can lead to predictable but false "failures" during certain aircraft maneuvers. Setting the threshold too high can lead to undetected but real sensor failures. The selected threshold values were a function of quantization of sensor output, digital system noise, and aircraft maneuvers. Details of this algorithm can be found in Volume II of this report. The failure detection algorithms were executed at each

TABLE 3.- SIRU NAVIGATION PERFORMANCE

Flight date	Navigation duration, sec	Maximum position error, n. mi.	Average position error, n. mi.	Average slope, n. mi./hr	Straight line (a+bt)	
					a, n. mi.	b, n. mi./hr
5/20	5,171	5.93	3.19	4.61	-0.02	4.65
5/30A	2,380	12.82	4.47	9.80	-12.31	34.56
5/30B	5,980	41.02	17.76	20.77	-6.56	26.59
6/16A	3,074	23.08	12.30	29.61	-2.95	34.73
6/16B	2,321	3.55	.81	2.70	-.15	3.06
6/18	15,303	33.99	12.60	5.49	4.39	3.90
6/25	3,405	12.94	7.63	15.58	1.07	13.86
7/14	6,005	35.59	15.65	19.79	-3.77	23.27
7/17A	4,888	4.40	2.52	2.94	.53	2.44
7/17B	4,155	2.10	1.02	1.22	.45	.77
7/24A	2,400	2.79	1.21	3.64	-.01	3.67
7/24B	2,555+	1.23+	.36	.97	.04	.88
7/24C	2,587+	4.04+	1.48	4.35	-.62	5.63
7/29A	4,900	14.06	8.53	10.50	-1.88	12.50
7/29B	2,426	7.13	1.76	6.14	-1.32	9.09
8/22A	2,630	2.93	1.38	3.94	-.24	4.44
8/22B	2,110	.36	.31	.84	.27	.14
8/22C	4,082	11.16	2.22	4.81	-.92	6.20
8/22D	?	?	?	?	?	?
8/29A	2,620	7.65	2.10	6.65	-1.48	9.71
8/29B ^a	2,501 ^a	.3 ^a	.15	.36	.12	.11
9/05A	2,200	2.50	1.06	3.56	-.10	3.81
9/05B	3,067	3.72	1.05	2.73	-.53	3.66
9/05C	2,013	1.86	.60	2.25	-.16	2.68
9/05D	2,053	3.00	.73	4.13	-.57	6.22
9/10A	3,733	3.97	1.19	2.36	-.20	2.65
9/10B	6,685	10.19	4.40	5.32	-1.92	6.86
9/10C	9,620	19.36	6.70	5.37	-1.66	6.29
9/10D	12,130	20.14	8.16	5.15	-.85	5.53
9/18A	3,860	6.22	2.22	4.52	-.96	5.85
9/18B	7,345	7.62	4.00	3.85	.34	3.61
9/18C	10,700	6.88	4.33	2.59	2.03	1.57
9/18D	1,600	2.91	.95	4.79	-.54	6.61
9/24	15,819	7.80	3.92	1.59	1.68	1.02

^aPosition reset at 1300 sec.

inertial data (gyro or accelerometer) update point to enable "failed" instruments to be taken off-line without causing excessive perturbation to the computed aircraft attitude or velocity. For the flight test program, the SIRU update rate was 20 times per second.

Scheduled sensor "failures" were imposed on 11 of the flight test segments by purposely miscompensating a sensor's null bias. Table 4 summarizes the results of the recorded in-flight scheduled failure tests of the FDI capability. The level of failure shown is the amount by which the null bias of the sensor was shifted in the test. The levels shown in the table are from Draper Laboratory flight records which were not recorded on the flight tape.

TABLE 4.- SCHEDULED FAILURE DETECTION/ISOLATION TEST RESULTS

Flight segment	Flight cond. (a)	Failed sensor	Failure level	Time in sec	Time detected sec	Undetected duration, sec	Error, δ Ang, δ V
7/17B	SL	C gyro	5°/hr	807	866	59	0.082°
	M	A gyro	10°/hr	1267	1300	33	.092°
7/24B	SL	C accel.	2 cm/sec ²	1628	1648	20	.40 m/sec
	SL	E accel.	3 cm/sec ²	2102	2123	21	.63 m/sec
7/24C	SL	C gyro	5°/hr	1392	1443	51	.071°
	SL	C accel.	2 cm/sec ²	1599	1619	20	.40 m/sec
	M,SL	A gyro	3°/hr	1808	1925	117	.097°
7/29A	M,SL	C gyro	3.5°/hr	1308	1394	86	.084°
	SL	D gyro	3°/hr	1433	1568	135	.112°
7/29B	M	C gyro(A)	0.5°/hr	607	---	---	---
	M	C gyro(B)	1.5°/hr	659	902	243	.101°
8/22B	SL	A gyro	6167°/hr	495	495	≤1	(.086°, 1.7°)
	SL	B gyro	6167°/hr	516	516	≤1	(.086°, 1.7°)
	M	A gyro	6167°/hr	1664	1664	≤1	(.086°, 1.7°)
	M	B gyro	6167°/hr	1682	1682	≤1	(.086°, 1.7°)
8/29B	SL,M	A gyro	6°/hr	675	775	100	.167°
	SL	B gyro	24°/hr	680	691	11	.073°
9/05A	SL	E gyro	6°/hr	1205	1254	49	.082°
	SL	F gyro	24°/hr	1211	1222	11	.073°
9/05B	M	A accel.	1 cm/sec ²	765	863	98	.98 m/sec
	M	B accel.	4 cm/sec ²	773	863	90	3.6 m/sec
9/05C	M	E gyro	6°/hr	595	645	50	.083°
9/05D	M	C accel.	1 cm/sec ²	488	572	84	.84 m/sec
	M	D accel.	4 cm/sec ²	500	572	72	2.88 m/sec

^aSL: straight-and-level flight; M: maneuvering flight.

In table 4, "Time In" is the SIRU navigation time point at which a recorded keyboard entry indicated that the "failure" was inserted; this assumes no appreciable lag in changing the compensation. "Time Detected" is the navigation time point at which the failure status flags showed the correct sensor to have failed. "Undetected Duration" is the time interval during which the undetected failure was corrupting the attitude and navigation calculations. The notations " ΔAng " and " ΔV " are resultant angle and velocity errors computed by multiplying the level of failure by the undetected duration. (Note: Approximately one-half of ΔAng or ΔV corrupts the attitude and navigation calculations because of the way hexad measurements are reduced to triad data in SIRU. Attitude and navigation errors are generally quite predictable from ΔAng and ΔV .)

The gyro error detection threshold was set to $1.14^\circ/\text{hr}$ from considerations of minimizing operational false alarms during flight. The "detection threshold" is directly related to sensor random errors, uncompensated modeling errors, and dynamic digital system noise.

The table shows that in every case but one the scheduled failed sensor was correctly isolated by the FDI algorithms even though unscheduled failures were present in many instances. In the one unsuccessful case, $0.5^\circ/\text{hr}$ null bias shift was inserted into the A computer's compensation of the C gyro (x, y plane) during flight segment 7/29B and went undetected. The angle error, Ang, may be seen to be approximately constant in all cases except the computer failures of flight segment 8/22B. In that test, data reduction of the flight tape could not pinpoint the detection duration within 1 sec. If the failure were detected immediately, no angle error would result. If it were detected in 0.05 sec (SIRU's computation update cycle), the error would be 0.0856° , and if detection required 1 sec, the error would be 1.7° .

Figure 8 shows both the theoretical experimental failure detection and isolation of the attitude sensors as a function of failure magnitude. Also indicated in figure 8 are flight control application requirements of which inertially smoothed landing guidance requires the shortest failure identification and removal time.

As indicated in table 2, there were many unscheduled failures during the flights. The details of these failures are found in Volume II of this report. These failures were caused by the following:

1. Improper sensor compensation
 - Human error
 - Calibration procedure
 - Poor error model
2. Thermal conditions
 - Blowing cold air
 - Ambient temperature in excess of 88°F
3. Other

The above failure sources were largely removed as the flight program progressed.

The statistical portion of the FDI algorithm was removed after Flight 7/17B because its operation was correlated with a high level of false alarms. The FDI algorithm will identify deficiencies in dynamic modeling errors by indicating a "failure" in the system. In order to reduce such false alarms, it would be necessary to increase the operating failure threshold to be compatible with system dynamics of the flight environment. The maximum values of the gyro error measured in flight are compared with those found in the laboratory in the following table.

	Flight	Laboratory
Turns	2.88°/hr	0.24°/hr
Level flight	1.0°/hr	0.01°/hr

Thus, considerable improvement in the aircraft dynamic modeling is required before flight failure thresholds can be lowered to those obtained in the laboratory.

Hardware and Software Limitations

During flight tests in the CV-340 aircraft, certain limitations were experienced with respect to the SIRU hardware and software. These limitations are now summarized.

Hardware limitations- The SIRU integrating rate gyro (IRIG 18 Mod B) was designed for continuous operation in a spacecraft environment. Because of the operational safety requirement to turn the system off when unattended, gyro parameter shifts were encountered across cooldown and powerdown; this necessitated frequent calibrations. The quantization level of 44 arc-sec was adequate for long-term space missions with periodic external updates, but not for the short-term high-dynamic environment of the aircraft. The rate limitation of 1 rad/sec is no problem in a spacecraft, but does represent a limitation in an aircraft. A 2-hr warmup requirement prior to a 2-hr calibration is no problem in the long countdown of a spacecraft but is definitely unacceptable for an operational aircraft.

The accelerometer (16 PM PIP) and its torque loop were more than adequate in all respects in the aircraft environment and therefore posed no limitation. Their calibration was stable over a period of 1 year.

The SIRU sensor pallet mounting fixture was designed to permit calibration of the SIRU sensors in the aircraft. It provided positioning of the inertial frame package to four cardinal points: 90° rotations about the system Z axis and one 90° rotation to put the Z axis in the vertical or horizontal plane. This permitted placing the ±X, ±Y, and +Z axes down individually for multiple position calibration. The mounting fixture did not allow a -Z axis down orientation. This missing sixth position would have improved the calibration accuracy.

A pair of wedge rings was provided to permit leveling the system prior to the aided single or multiple position test; however, the aircraft was off level more than these rings could compensate. It was necessary to jack up the nose of the aircraft by about 3° to put the sensor level within the compensation range of the wedge rings.

The sensor level was measured by a 10-arc-sec bubble mounted on the SIRU frame in a recessed well so that it could be rotated 360° . The 10-arc-sec bubble mounting surface had been precision-machined with respect to the system reference cube. With repeated operations, its aluminum surface became worn and the repeatability of the measured accelerometer biases was uncertain.

The SIRU sensor pallet cooling system was limited to an ambient air temperature range of $+40^\circ$ to $+88^\circ$ F. The inertial component temperature controllers could not control the gyro and accelerometer temperatures outside this range. Lack of control caused sensor parameter shifts which would be detected by the FDI software as a transient sensor failure. The aircraft air conditioning system was inadequate in the early part of the flight test program and allowed ambient air temperatures to exceed 90° . It was never adequate when the aircraft was sitting on the ground and the outside air temperature exceeded 90° . Operation of the air conditioning required that one engine be running. This limited the accuracy of the calibration. The ground-support cooling system used to correct this problem caused overcooling of some inertial components when the cabin temperature was normal because the outlets of the aircraft air conditioning were exhausting cold air directly onto these inertial components, causing uncompensated temperature gradients in the sensors and thereby triggering a transient failure report from the FDI algorithm. This condition was corrected once the source of the problem had been isolated.

Software limitations- Postflight analyses indicated that the base motion isolation software mechanization did not perform as well as expected and was the cause of excessive errors in estimates of north and level during fine alignment.

Using computed body velocity at the end of each 1-sec navigation update to approximate the average velocity over that update period caused acceleration-induced position errors as large as 52 m for 180° turns. These errors averaged to zero for straight-line acceleration and deceleration.

The statistical FDI algorithm threshold limits were specified to be 1.5 times the standard deviation of the gyro error derived from the laboratory test environment. Flight test experience showed that the gyro errors were greatly increased as compared to the laboratory dynamic test data. The original limits were $0.06^\circ/\text{hr}$ for static conditions and a maximum dynamic increase of $0.12^\circ/\text{hr}$ to give a maximum threshold of $0.18^\circ/\text{hr}$. These were changed to $0.48^\circ/\text{hr}$ static and $0.96^\circ/\text{hr}$ maximum dynamic increase to give a maximum threshold of $1.44^\circ/\text{hr}$. These increases were derived more intuitively than analytically and proved to be inadequate as evidenced by the large number of "false" failures. The software was then modified to remove the statistical FDI in the navigation mode and therefore in the flight mode (after flight 717). The FDI algorithm was then totally dependent upon the TSE which had thresholds

of 1.14°/hr MASE and 1.48°/hr maximum dynamic increase to give a maximum threshold of 2.62°/hr. Later analysis showed that the statistical limits should have been 0.75°/hr static with a maximum dynamic increase of 1.65°/hr to give a maximum threshold of 2.50°/hr for utilization of the statistical FDI during aircraft navigation.

The TSE failure detection thresholds were initially determined on the basis of laboratory tests without compensation for aircraft dynamics. However, the TSE threshold is environmentally sensitive. The initial gyro threshold was 0.76°/hr with a maximum dynamic increase of 0.81°/hr, resulting in a maximum threshold of 1.57°/hr. Early flight test data indicated false gyro "failures" were being triggered during aircraft turn maneuvers because these limits were low. The limits were raised to 1.14°/hr for the threshold and 1.98°/hr for the maximum dynamic increase, giving a maximum threshold of 3.12°/hr. Also, the accelerometers, initially set at 0.4 cm/sec² for the first-fail threshold and 0.13 cm/sec² for the second-fail threshold were reset to 0.28 and 0.25 cm/sec², respectively. These changes removed the false failure indications during aircraft maneuvers.

CONCLUSIONS

The following conclusions have been drawn from the program test results relative to each of the three principal objectives presented previously.

Navigation System Performance

For short-haul aircraft operations, free-inertial navigation accuracy of 1 to 3 n. mi./hr is generally acceptable. Test results showed that this performance level was achieved during cruise conditions. Navigation performance during terminal area maneuvers (including degradation in the presence of scheduled and unscheduled failures) produced higher error buildup. However, even without preflight calibration, these error rates did not exceed 5 n. mi./hr. In summary, it was demonstrated that a system like SIRU can provide the inertial navigation capability necessary for short-haul applications. However, additional analysis, software design, and testing are required to minimize dynamic errors resulting from uncompensated instrument misalignments and scale factor errors.

The SIRU Navigation Analysis Program was modified to allow computation of navigation states by inertially smoothing DME radio data. An analysis of SIRU's potential for providing inertially smoothed radio navigation (i.e., aided-inertial navigation) indicated that a DME/baroaltimeter/inertial system based on SIRU could easily maintain a navigation accuracy of a few hundred meters. For one flight, the maximum aided-inertial root-sum-square position error was about 0.2 n. mi. compared to a free-inertial maximum error of 3.7 n. mi. on the same flight.

As an auxiliary effort, some sensor data from the flight test program were analyzed to assess SIRU use for integrated short-haul flight control applications. The SIRU gyro resolution was 44 arc-sec (0.0002 rad) per bit. Data analyses showed that the quantization-derived digital noise from the 44-arc-sec/bit resolution would prohibit use of such data in short-haul flight control systems. Also, the system's full-scale gyro measurement capacity of 1 rad/sec is too low for many flight control applications. Scale changing to achieve higher full scale without increasing the word length would increase the quantization error. Current flight control technology can produce 1.6 arc-sec quantization at 2 rad/sec full-scale output. Thus, substantial modification to both hardware and software of SIRU would be required to allow flight control use.

Failure Detection and Isolation Algorithm Performance

The analysis of the flight data was directed towards comparing the experimentally measured failure isolation time with the theoretical isolation time. This comparison is related to the digital system noise derived from motion dynamics. Its assessment provides technical insight for assessing other redundancy management strategies for short-haul avionics.

The torque rebalance loops used in SIRU (dictated by Apollo technology) were tailored to 44 arc-sec angular resolution for the original spacecraft application. This size was too large for aircraft operations. Included in figure 8 is a theoretical 1.6-arc-sec resolution (available in current inertial navigation system technology) plot of attitude failure rate versus failure identification and removal time. Such resolution would provide considerably better results.

A redundant strapdown system should be able to isolate a navigation error of 28 n. mi. in 4 hr (trans-Atlantic criterion) which corresponds to approximately a constant $0.1^\circ/\text{hr}$ attitude failure rate. The SIRU flight experiments showed that achieving a $0.1^\circ/\text{hr}$ failure detection and isolation is more difficult than originally projected for aircraft operations. It was not possible to isolate sensor failures smaller than $1.6^\circ/\text{hr}$ because the detection threshold had to be adjusted to a higher value to avoid false alarms. This threshold was approximately a factor of 30 larger than the laboratory sensor drift measurement. This experimentally measured threshold indicated that the SIRU system can detect and isolate only hard failures for inertial navigation but may provide reliable operation for flight control purposes.

In reviewing these results, it must be remembered that the SIRU concept was originally designed as a redundant strapdown replacement for the Apollo spacecraft gimbaled inertial measurement unit. The resulting operational, electrical, mechanical, environmental, and mission interface requirements were distinctly different from those which existed in the CV-340 aircraft.

The flight test results have shown the limitations of the existing SIRU hardware and software design for short-haul transportation application. The results point out areas where additional design and verification efforts are

required before a redundant strapdown system can be considered for operational usage. The fault detection and isolation capability is the area in need of the most work if the SIRU concepts are to become applicable for short-haul aircraft.

Dual Computer System Reliability

The design of the SIRU dual computer system is basically a good one from the standpoints of both correctness and reliability. Its strong points are the intermodule isolation, the intercomputer communication protocol, the wide variety of error detectors, and the effectiveness of the arbiter function. The SIRU computer arrangement also has several weak points which do not affect the normal operation of the system, but do suggest design improvements which could improve the overall reliability and maintainability of future systems. These include the self-tests as applied to failure recovery, the computer software structures, the preflight test facilities, the use of different components, and an extension of the arbiter function (refs. 7 and 8). Elaboration on each of these points is presented in Volume II of this report.

The principal difficulty with the SIRU dual computer system is the inability to correct for transient faults which "reprogram" the computer memory (i.e., an intermittent connection in a "sense" or "write" amplifier) or the occurrence of multiple faults. When the transient fault is inactive after modifying memory, the computer self-diagnostic routines will incorrectly recertify it, but the arbiter will show computer disagreement and no method of identifying the correctly programmed computer.

The SIRU preflight test system was designed in such a way that the parity checker, the bit-correct, and the clock-active error detectors could not be adequately tested. Details for necessary preflight testing and how system improvements could be made are also discussed in Volume II of this report.

REFERENCES

1. Eberlein, A. J.; and Savage, P. G.: Strapdown Cost Trend Study and Forecast. NASA CR-137585, 1974.
2. Gilmore, J. P.; and Cooper, R. J.: SIRU Development - Final Report. Vol. 1. System Development. CSDL R-747, Charles Stark Draper Laboratory, July 1973.
3. Musoff, Howard: SIRU Utilization. Vol. 1. Development and Test Evaluation. CSDL R-746, Charles Stark Draper Laboratory, March 1974.
4. Booth, Robert A.; Gilmore, Jerold P.; and Hruby, Ronald J.: Test Results and Flight Preparation for the Strapdown Redundant Inertial System. Institute of Navigation Annual Meeting, June 1974.
5. Booth, Robert A.; and Shuck, Thomas L.: SIRU Flight Test Readiness Final Report. CSDL R-934, Charles Stark Draper Laboratory, 1975.
6. Ressler, Bruce E.: Design of a Dual Computer Configuration for Redundant Operation. CSDL T-586, Charles Stark Draper Laboratory, June 1973.
7. Wakerly, J. F.; and McCluskey, E. J.: Design of Low-Cost General Purpose Self-Diagnosing Computers. Proceedings of the IFIP Congress, 1974, Stockholm, Sweden, 1976, pp. 108-111.
8. King, J. E.: Proving Programs Correct. IEEE Trans. Computers, vol. C-20, 1971, pp. 1331-1336.

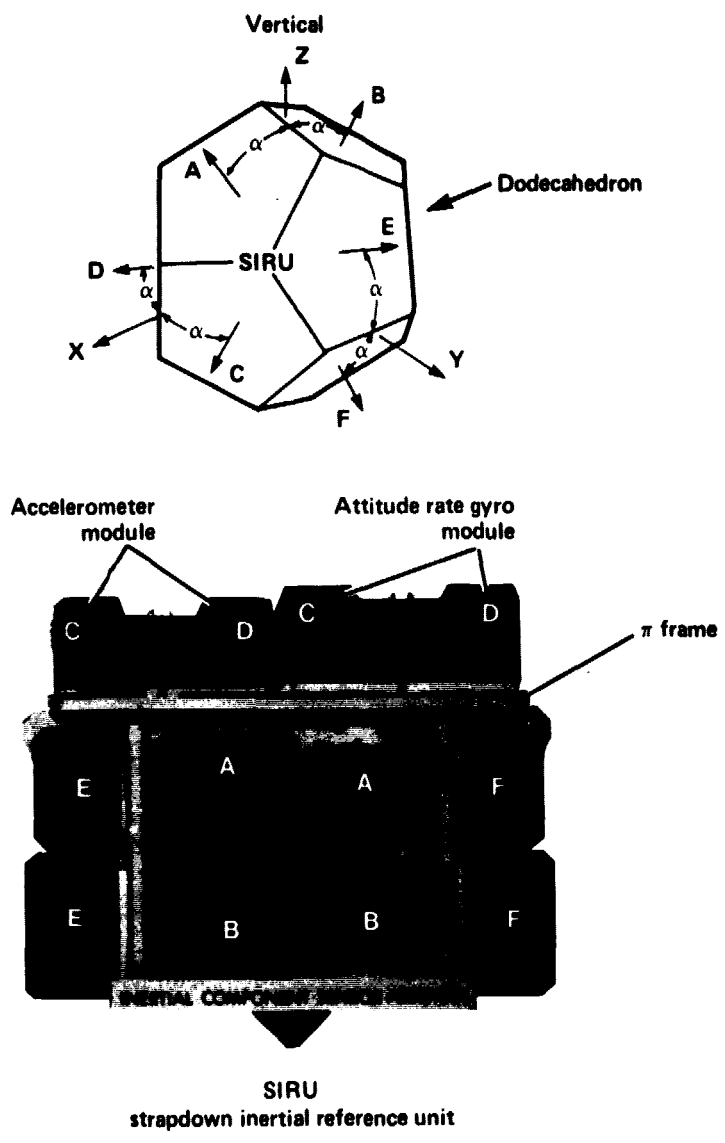


Figure 1.- Flight test orientation of SIRU dodecahedron hexad.

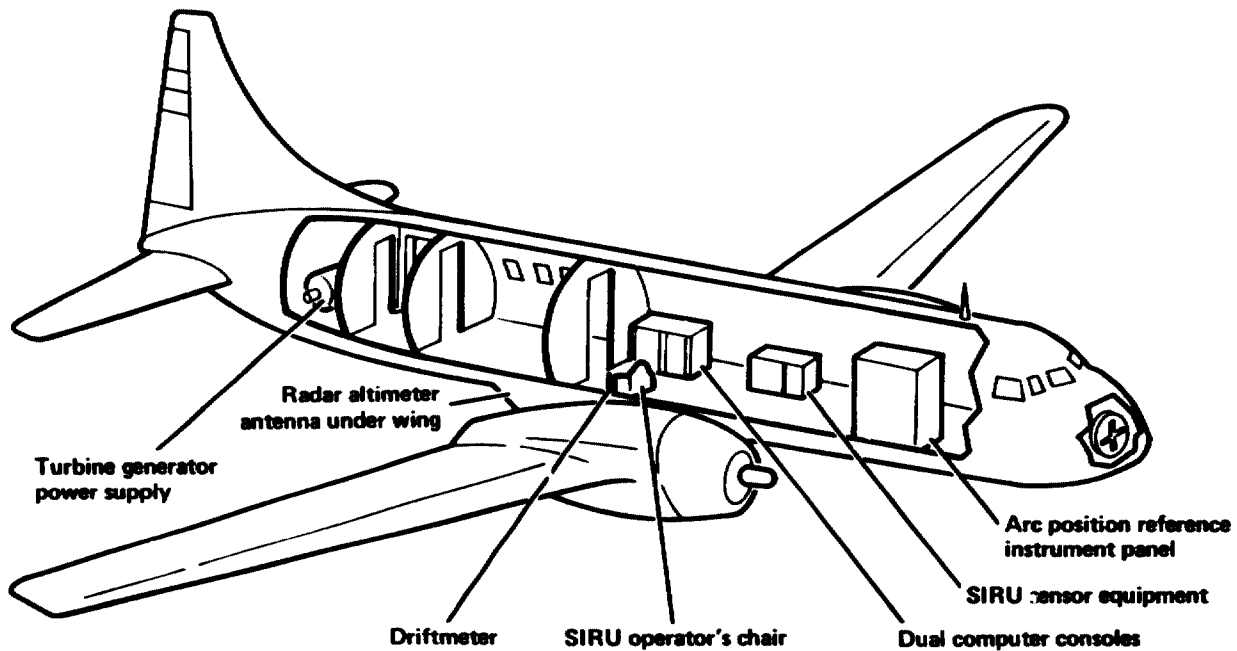


Figure 2.- Ames Research Center CV-340 test aircraft with SIRU system installed.

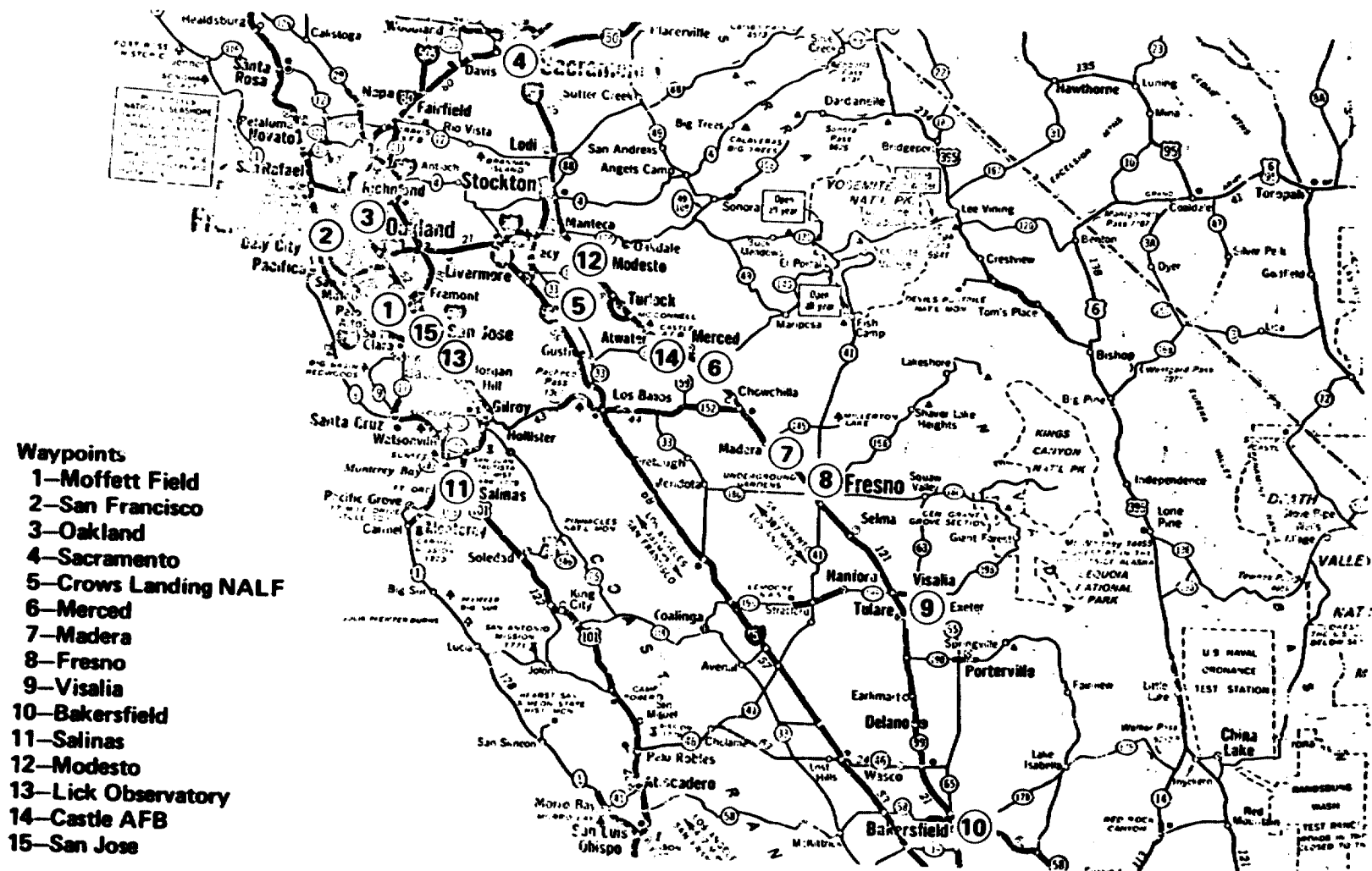


Figure 3.- Visual landmarks for the CV-340 flight test.

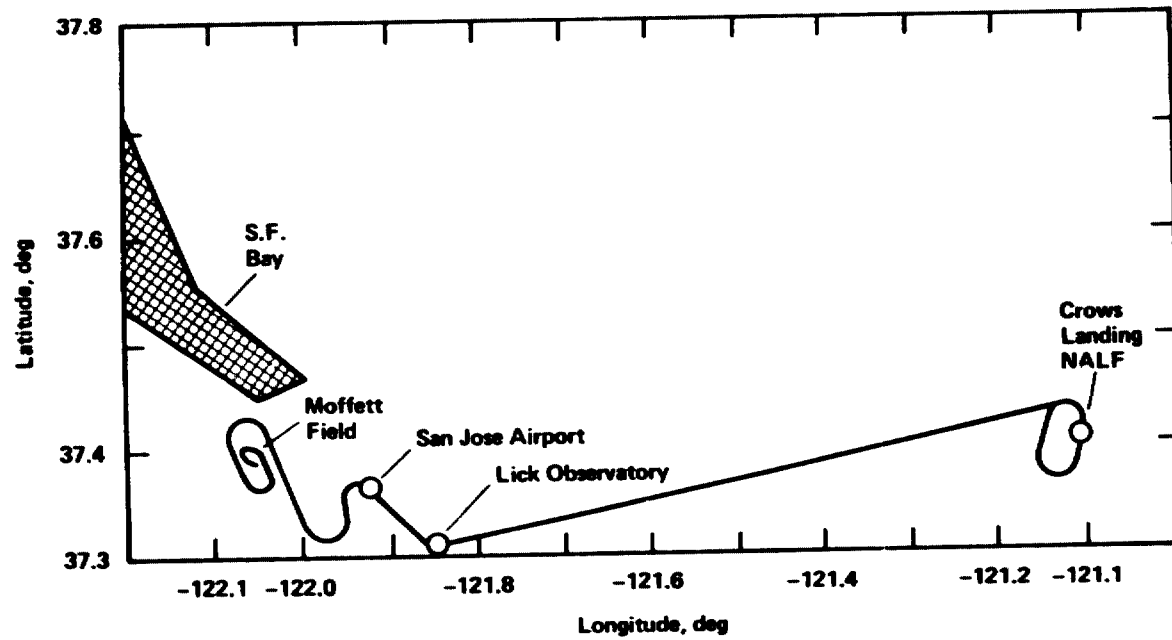


Figure 4.- Flight sequence - Moffett Field to/from Crows Landing NALF.

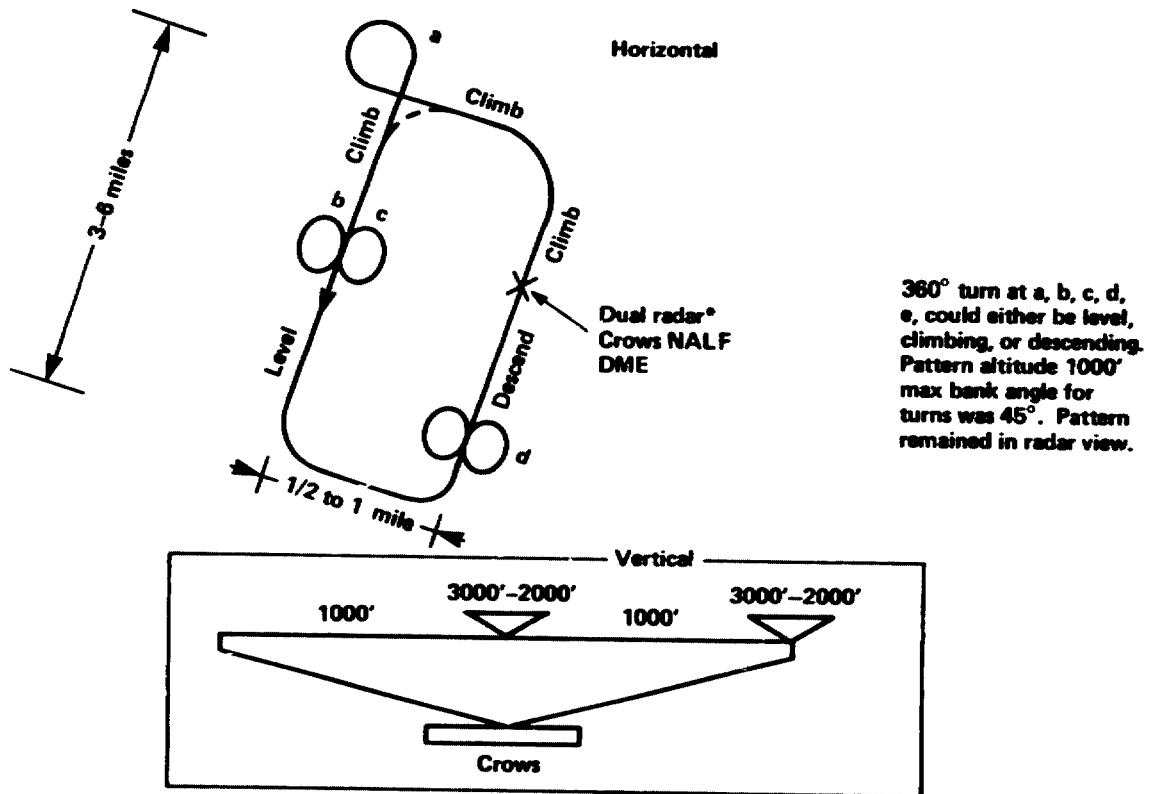


Figure 5.- Terminal area pattern near Crows NALF.

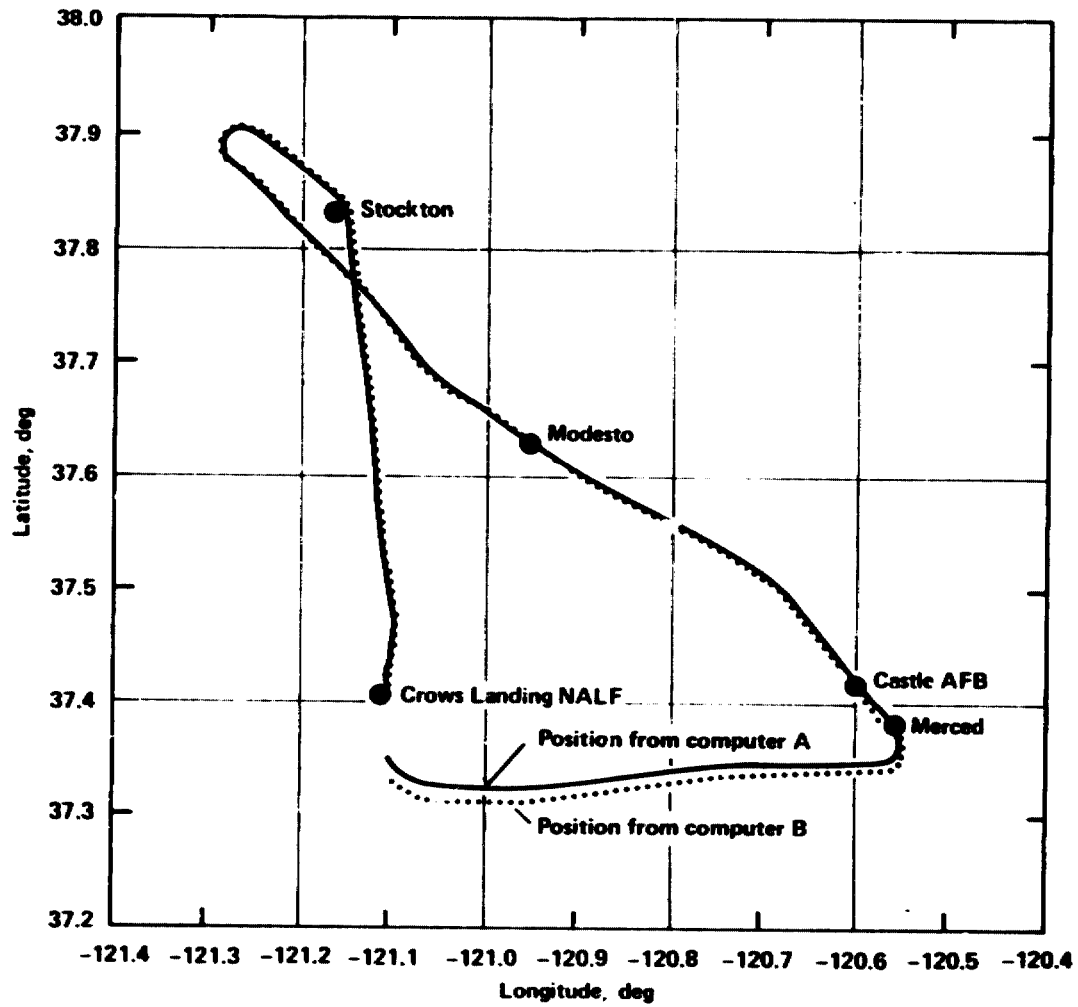


Figure 6.-Typical flight sequence originating at Crows Landing NALF.

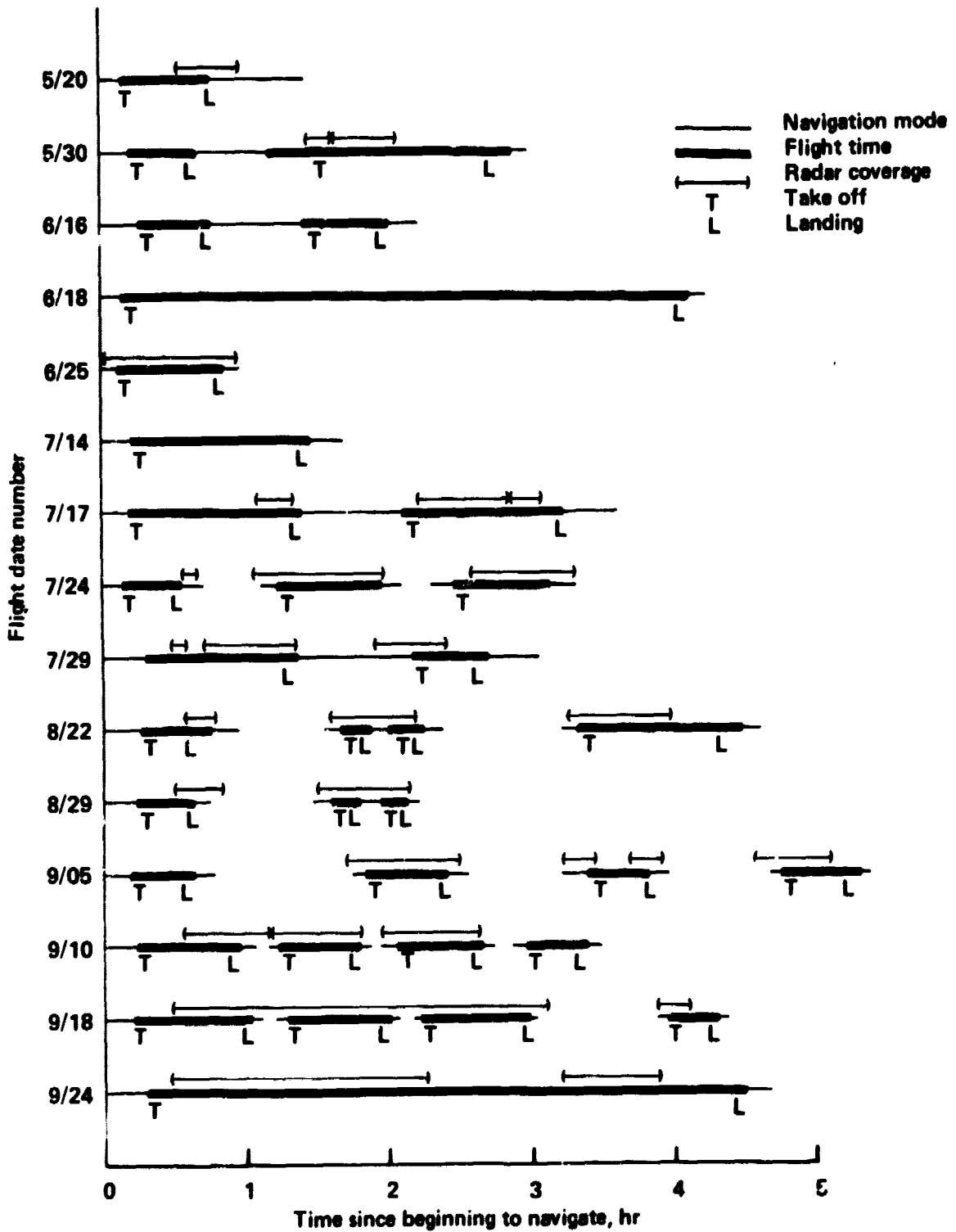


Figure 7.- SIRU flight duration and radar coverage.

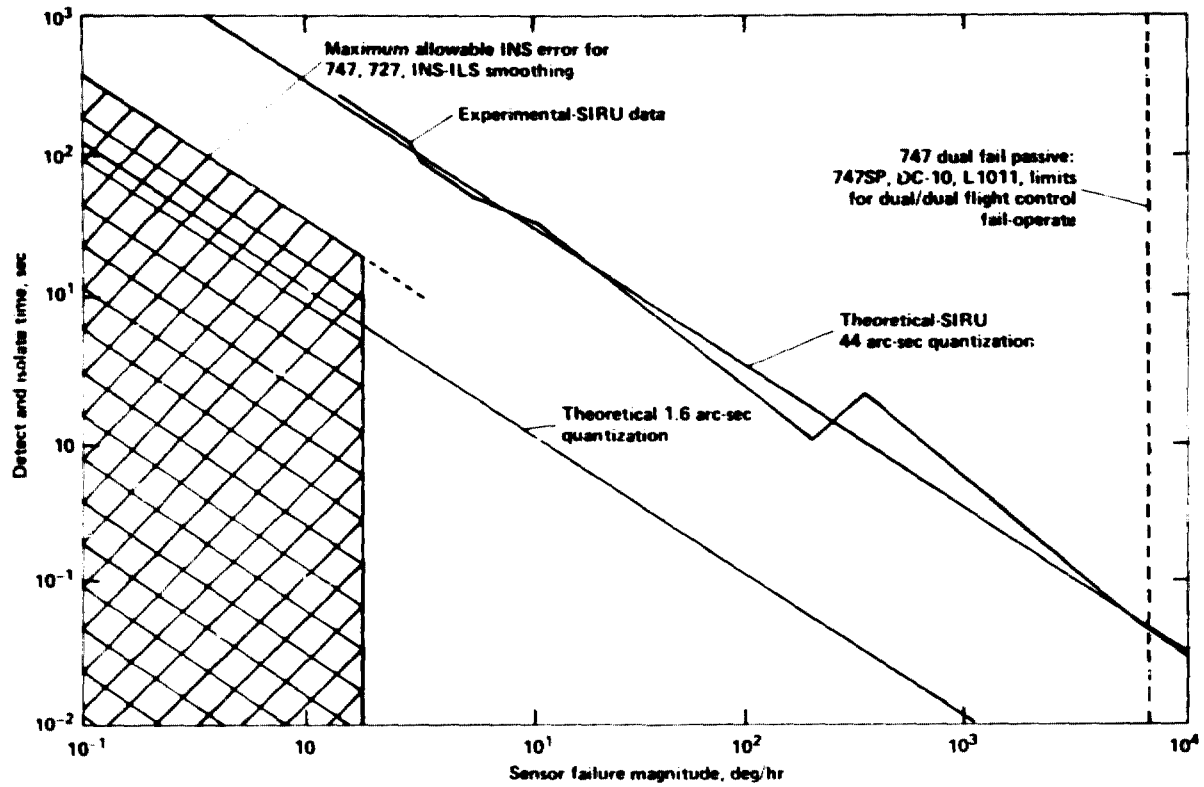


Figure 8.- Scheduled SIRU failure detection and isolation flight test performance summary.